

Study of reaction $\pi^- A \rightarrow \pi^+ \pi^- \pi^- A$ at VES setup.

Igor Kachaev for VES Collaboration. ¹

Department of Hadron Physics, IHEP, Protvino, Russia, 142284

Abstract.

The results on partial wave analysis of 3π system in reaction $\pi^- A \rightarrow \pi^+ \pi^- \pi^- A$ at the momentum 36.6 GeV/c on the beryllium target are presented. New method of amplitude analysis is suggested — extraction of largest eigenvalue of density matrix. Exotic wave with $J^{PC} = 1^{-+} \rho\pi$ is studied in four t' regions. No narrow object around $M = 1.6$ GeV/c² is found. Unusually steep t' dependence for $\pi(1300)$ object is detected.

INTRODUCTION. THE PARTIAL WAVE ANALYSIS.

The VERtEX Spectrometer (VES) setup is a large aperture magnetic spectrometer including the system of proportional and drift chambers, a multichannel threshold Čerenkov counter, beam-line Čerenkov counters, a lead-glass γ -detector (LGD) and trigger hodoscope. This permits full identification of multi-particle final states. The setup runs on the negative particle beam with the momentum of 36.6 GeV/c. The description of the setup can be found in [1].

In this report we present some results of partial wave analysis of the 3π system in the reaction $\pi^- Be \rightarrow \pi^+ \pi^- \pi^- Be$ for different t' regions $|t'| = 0.01 - 0.07 - 0.15 - 0.30 - 0.80$ GeV²/c². The discussed results are based upon the statistics of about $8.0 \cdot 10^6$ events. Our previous results were published in [2].

The PWA has been performed in the 0.8–2.6 GeV/c² mass region in 50 MeV bins for different t' regions. Modified version of the Illinois PWA program [3] with maximum likelihood method has been used for the analysis. Amplitudes were written using isobar model and relativistic covariant helicity formalism according to [4]. Explicit t' -dependence $f(t) = te^{-bt}$ was included for waves with nonzero projection of spin on GJ z-axis. Density matrix of full rank was used to describe final state. The set of 42 partial waves in the form $J^P L M \eta$ isobar [3] was used in the analysis. Full wave set and parameterization of isobars including special treatment of $\pi\pi$ S-wave can be found in [2]. For the channels with $J^{PC} = 0^{-+}, 1^{++}, 2^{-+}$ largest waves are assigned to their own density matrix elements and are enabled to freely interfere with each other.

¹ Amelin D.V., Dorofeev V.A., Dzhelyadin R.I., Gouz Yu.P., Kachaev I.A., Karyukhin A.N., Khokhlov Yu.A., Konoplyannikov A.K., Konstantinov V.F., Kopikov S.V., Kostyukhin V.V., Kostyukhina I.V., Matveev V.D., Nikolaenko V.I., Ostankov A.P., Polyakov B.F., Ryabchikov D.I., Solodkov A.A., Solovianov O.V., Zaitsev A.M.

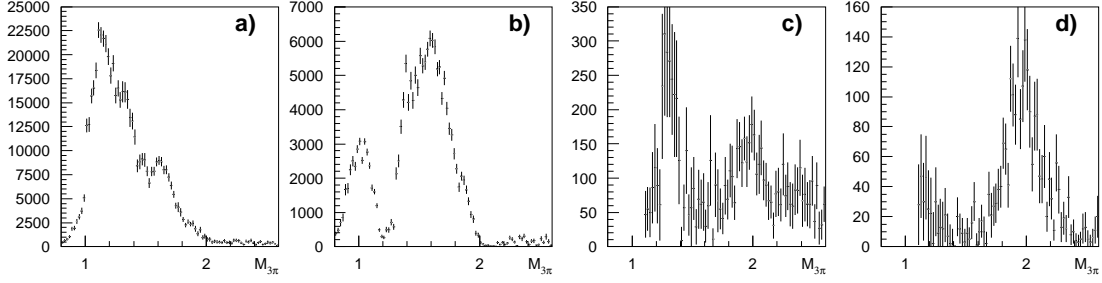


FIGURE 1. Wave $2^-P0^+\rho\pi$ at $|t'| < 0.03 \text{ GeV}^2/c^2$ in a) full density matrix, b) largest eigenvalue; wave $4^+G1^+\rho\pi$ at $|t'| < 0.03 \text{ GeV}^2/c^2$ in c) full density matrix, d) largest eigenvalue.

EXTRACTION OF LARGEST EIGENVALUE.

Results of PWA are represented in general by *density matrix*. For physical analysis *amplitudes* are much more convenient. We present here a new type of amplitude analysis — extraction of largest eigenvalue of density matrix. Density matrix can be represented by its eigenvalues and eigenvectors:

$$\rho = \sum_{k=1}^d e_k * V_k * V_k^+ \quad \text{where} \quad \begin{cases} e_k \text{ is } k\text{-th eigenvalue, } e_1 > e_2 > \dots > e_d \\ V_k \text{ is } k\text{-th eigenvector} \end{cases}$$

Single out leading term:

$$\rho = \rho_L + \rho_S, \quad \rho_L = e_1 * V_1 * V_1^+, \quad \rho_S = \sum_{k=2}^d e_k * V_k * V_k^+$$

Here ρ_L is coherent part of density matrix and ρ_S is the rest (incoherent part). To be of physical meaning, this decomposition must be *stable* with respect to variations of density matrix elements. This is so if eigenvalues are *well separated* in comparison with errors in ρ matrix: $|e_1 - e_2| \gg \sigma(\rho_{ij})$. This is the case for $\pi^+\pi^-\pi^-$ where $e_1 \sim 1, e_2 \sim 0.1$.

Extraction of largest eigenvalue has the following advantages. By construction matrix ρ_L has rank one, so phases are well defined. It quantitatively uses information about coherence factors, which is often ignored. Practical experience shows that resonance structures tend to concentrate in ρ_L and leakage (see below) is suppressed in ρ_L . Nevertheless, ρ_S can contain different non-leading exchanges, albeit it often contains garbage. We can also note that if the wave is small in ρ_L , its phase with respect to largest waves can not be measured.

As a restriction this method requires a lot of data for good fit with small errors. It is not applicable if eigenvalues are not separated. In this case sometimes a group of clustered eigenvalues can be extracted. It is also not applicable if all eigenvalues except one are not statistically significant, as it is the case for unnatural sector for $\pi^+\pi^-\pi^-$ system.

An example of separation of largest eigenvalue is present in figure 1. On sub-figures a) and b) one can see a huge difference between wave $2^-P0^+\rho\pi$ in the full density matrix and in the largest eigenvalue. It was already noted [5, 2] that at low t' region this wave is large and highly incoherent with others at $M_{3\pi} \approx 1.2 - 1.4 \text{ GeV}/c^2$ and have

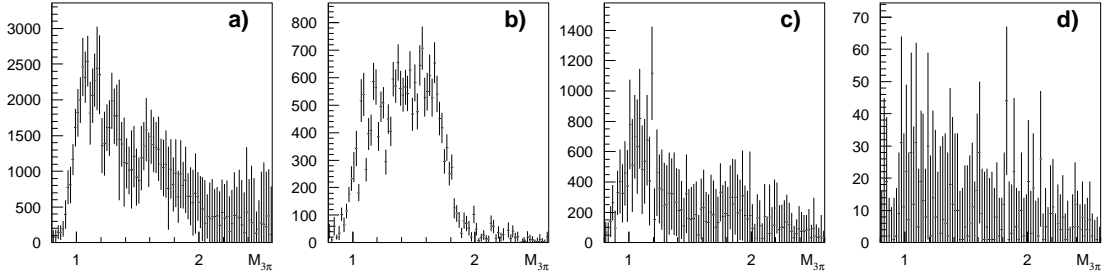


FIGURE 2. Leakage study. Wave $1^{-+}\rho\pi$ at $0.03 < |t'| < 1.0 \text{ GeV}^2/c^2$ in: a) real data, full ρ matrix; b) real data, largest eigenvalue; c) leakage, full ρ matrix; d) leakage, largest eigenvalue.

only a relatively small shoulder at $M_{3\pi} \approx 1.6 \text{ GeV}/c^2$, which corresponds to well known $\pi_2(1670)$. Our analysis confirms this as shown in figure 1 a). Contrary to this in the largest eigenvalue this wave is dominated by physical $\pi_2(1670)$. The bump at low $M_{3\pi}$ is at least ten times suppressed, which is consistent with its low coherence with other waves. The physical nature of this phenomena is still unknown.

In figures 1 c), d) one can see the difference between full density matrix and largest eigenvalue for the wave $4^+G1^+\rho\pi$ at $|t'| < 0.03 \text{ GeV}^2/c^2$. At both figures we can see at $M_{3\pi} \approx 2.0 \text{ GeV}/c^2$ a signal for $a_4(2050)$ while in fig.1 c) we can also see a bump at $M_{3\pi} \approx 1.3 \text{ GeV}/c^2$ which is absent in fig.1 d). This bump is a leakage from $a_2(1320)$ with intensity about 0.2% of total number of events or about 7.5% of 2^+ wave in this low $|t'|$ region. This leakage is at least ten times suppressed in coherent part of density matrix.

LEAKAGE STUDY.

We have used the following method to study a possible leakage effects due to finite setup resolution and limited knowledge of setup acceptance. At first, we fit real data with small but representative wave set — 12 largest waves. The result of this step is a reasonably accurate representation of multidimensional distribution of real events. Next we generate Monte-Carlo events according to density matrix from this fit, smear these events according to modeled setup resolution and fit them as usual using standard wave set with all 42 waves. To study dependence of results of variation of modeled acceptance, we have used Monte-Carlo events without smearing, but used corrupted MC program (with hodoscope trigger logic excluded) for final fits with 42 waves.

The results of leakage study for exotic wave $1^{-+}\rho\pi$ are shown in fig. 2. One can see that exotic wave can contain 30–50% of leakage, but can not be described by leakage. The structure of density matrix in the real data and leakage is quite different — in the coherent part of ρ leakage is 20–50 times suppressed. Most other waves can contain 5–10% of leakage.

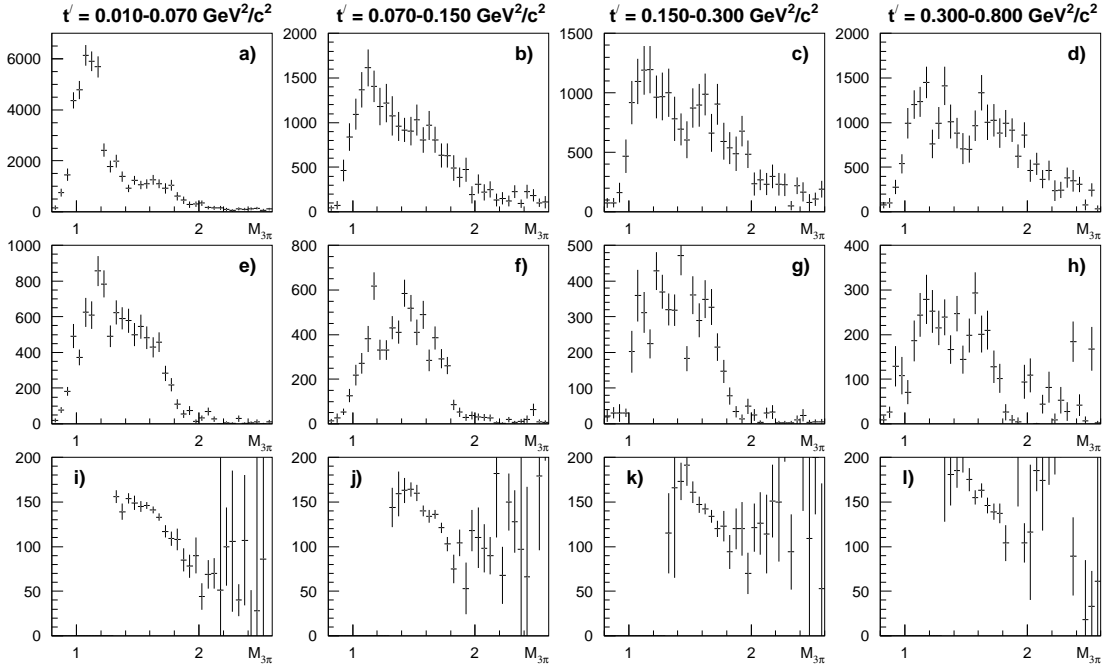


FIGURE 3. Wave $1^-P1^+\rho\pi$ at different $|t'|$ regions: a–d) full density matrix; e–h) largest eigenvalue; i–l) phase difference $\phi(1^-+\rho\pi) - \phi(2^-+f_2\pi)$, full density matrix.

WAVES WITH $J^{PC} = 1^{-+}$.

Waves with exotic quantum numbers $J^{PC} = 1^{-+}\rho\pi$ were included in our analysis with all possible projections $M^\eta = 1^+, 0^-, 1^-$. Waves with $M^\eta = 0^-, 1^-$ are small in comparison with $M^\eta = 1^+$ (except for $M_{3\pi} < 1.2 \text{ GeV}/c^2$) and are not considered by us as significant. Wave $1^-P1^+\rho\pi$ in four different t' regions is shown in fig. 3. In the full density matrix (fig. 3 a–d) at low t' this wave consists mainly of a bump around $M = 1.0 - 1.2 \text{ GeV}/c^2$ and a shoulder at $M \approx 1.6 \text{ GeV}/c^2$. At higher t' regions the bump diminishes while the shoulder remains approximately the same. From figures 3 e–h) one can see that this shoulder corresponds mainly to the coherent part of the density matrix, and this part remains stable over investigated t' region. The bins over t' are selected so that numbers of events in $a_2(1320)$ peak are approximately the same for all bins, namely about 20000 events/50 MeV, so t' distribution for coherent part of exotic wave is roughly the same as for $a_2(1320)$ while its crosssection is only 2–3% of it. One can see a sharp drop on the coherent part of exotic wave at $M_{3\pi} \approx 1.8 \text{ GeV}/c^2$. We can see analogous effect in some other $\rho\pi$ waves and it can be connected with worse description of high $M_{3\pi}$ region. Phase difference $\phi(1^-P1^+\rho(770)\pi) - \phi(2^-S0^+f_2(1270)\pi)$ is shown in fig. 3 i–l). This phase difference is not constant, visible drop corresponds to phase raise of $\pi_2(1670)$ resonance. Again the shape of phase variation is more or less stable over inspected t' region. In general we can not see here narrow exotic object with $M \approx 1.6 \text{ GeV}/c^2$.

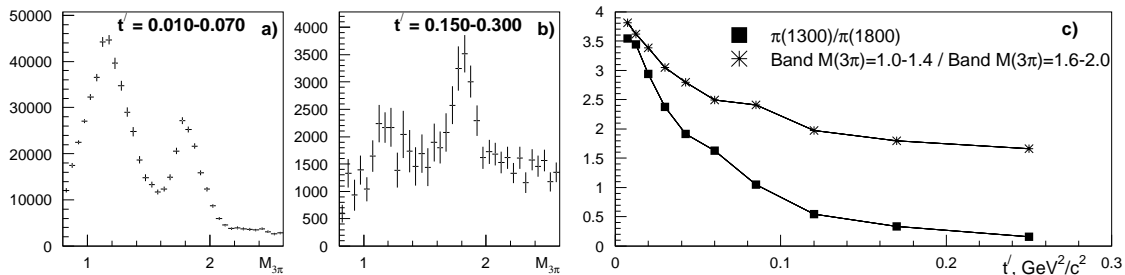


FIGURE 4. Wave $J^{PC} = 0^{-+}\epsilon\pi$: a) $|t'| = 0.01 - 0.07 \text{ GeV}^2/c^2$ region; b) $|t'| = 0.15 - 0.30 \text{ GeV}^2/c^2$ region; c) relative $|t'|$ dependence of $\pi(1300)/\pi(1800)$ signals and corresponding $M_{3\pi}$ bands.

WAVES WITH $J^{PC} = 0^{-+}$.

Results of PWA for the wave $0^{-+}S_0^+\epsilon\pi$ in different t' regions are presented in figure 4. At low t' two peaks are visible which corresponds to $\pi(1300)$ and $\pi(1800)$. At higher t' peak for $\pi(1300)$ is clearly suppressed. Relative strength of $\pi(1300)$ and $\pi(1800)$ signals together with relative number of events in $M_{3\pi} = 1.0 - 1.4 \text{ GeV}/c^2$ and $M_{3\pi} = 1.6 - 2.0 \text{ GeV}/c^2$ bands is shown in fig 4c) in ten t' regions. One can see that t' distribution for $\pi(1300)$ is much more steep than for $\pi(1800)$ or even for the total number of events in corresponding $M_{3\pi}$ band. A possible explanation of this phenomena can be given if the $\pi(1300)$ bump is at least partially non-resonant and produced by Deck-type final state scattering.

CONCLUSIONS.

Partial wave analysis of $\pi^+\pi^-\pi^-$ final state at different t' regions was performed on VES data. New type of amplitude analysis was suggested — extraction of the coherent part of density matrix. Its advantages and limitations were briefly discussed.

Wave $J^{PC} = 1^{-+}\rho\pi$ was studied in different t' regions $t' = 0.010-0.070-0.150-0.300-0.800 \text{ GeV}^2/c^2$. Wave shape is broad and more or less the same in all t' regions studied. Clear phase variation with respect to $\pi_2(1670)$ is visible in all t' regions. No narrow object around $M = 1.6 \text{ GeV}/c^2$ is found.

Waves $J^{PC} = 0^{-+}$ were studied in the same t' regions. Abnormally steep t' distribution for $\pi(1300)$ was established. This phenomena can be understood if $J^{PC} = 0^{-+}$ wave in $\pi(1300)$ region is partially consists of Deck-type background.

This work is supported in part by INTAS-RFBR 97-02-71017, RFBR 00-02-16555, RFBR 00-15-96689 grants.

REFERENCES

1. S.I. Bitukov et al., Phys. Lett., **B268**, 137 (1991).
2. D.I. Amelin et al., Phys. Lett., **B356**, 595 (1995).
3. J.D. Hansen et al., Nucl. Phys., **B81**, 403 (1974).
4. S.U.Chung, Phys. Rev., **D48**, N3, 1225 (1993).
F.Filippini et al., Phys. Rev., **D51**, N5, 2247 (1995).
5. C. Daum et al., Phys. Lett., **B89**, 285 (1980).